Guaranteed Minimization of the Bit Error Ratio for Correlated MIMO Systems

Ekaterina Auer and Andreas Ahrens
Department of Electrical Engineering, University of Applied Sciences Wismar, 23966 Wismar, Germany, {ekaterina.auer, andreas.ahrens}@hs-wismar.de

Abstract. The multiple-input multiple-output (MIMO) mechanism is a method to increase the capacity of communication links by employing multiple transmitting and receiving antennas. An important quality criterion for such systems is the bit error probability characterizing the bit error ratio (BER). If simple MIMO transmission channel and data source models are assumed, BER can be computed analytically and optimized with respect to major parameters it depends on. In this contribution, we consider BER minimization for MIMO links with uncertainty in their parameters under good and poor scattering conditions, illustrated by close-to-life simulation examples. The obtained results show that the achievable performance depends strongly on the number of active MIMO layers, the assigned transmit power per layer and the bits per number of transmitted symbols.

Keywords: methods with automatic result verification, BER, power allocation, bit allocation

1. Introduction

The strategy of placing multiple antennas at the transmitter and receiver sides, well-known as multiple-input multiple-output (MIMO) method, improves both the capacity and the integrity of wireless systems through the use of the spatial characteristics of the underlying channel (Foschini, 1996; Telatar, 1999). A simple linear stochastic model for a frequency flat MIMO link consisting of n_{T} transmitting and n_{R} receiving antennas is

$$\vec{y} = H \cdot \vec{a} + \vec{n}, \quad \vec{y}, \vec{n} \in \mathbb{C}^{n_{\mathrm{R}}},\ \vec{a} \in \mathbb{C}^{n_{\mathrm{T}}},\ H \in \mathbb{C}^{n_{\mathrm{R}} \times n_{\mathrm{T}}}\ , \tag{1}$$

where $\vec{y}$ is the received data vector, $\vec{a}$ is the transmitted signal vector, $\vec{n}$ is the vector of the additive white Gaussian noise at the receiver side with the zero mean and the variance σ^2 in both real and imaginary parts, and H is the channel matrix. The channel matrix organizes the individual descriptions of the paths from every transmit antenna to every receive antenna. In wireless communications, those paths are found to be appropriately simulated by the Rayleigh distribution. That is, for a frequency flat MIMO link, the paths' descriptions (the coefficients of the $(n_{\mathrm{R}} \times n_{\mathrm{T}})$ channel matrix H) are assumed to be independently and identically distributed Rayleigh fading channels (Sklar, 1997) with equal variance δ^2. This model can be easily extended to reflect frequency selective channel conditions (Raleigh and Cioffi, 1998). In this paper, however, we focus on the frequency flat case.

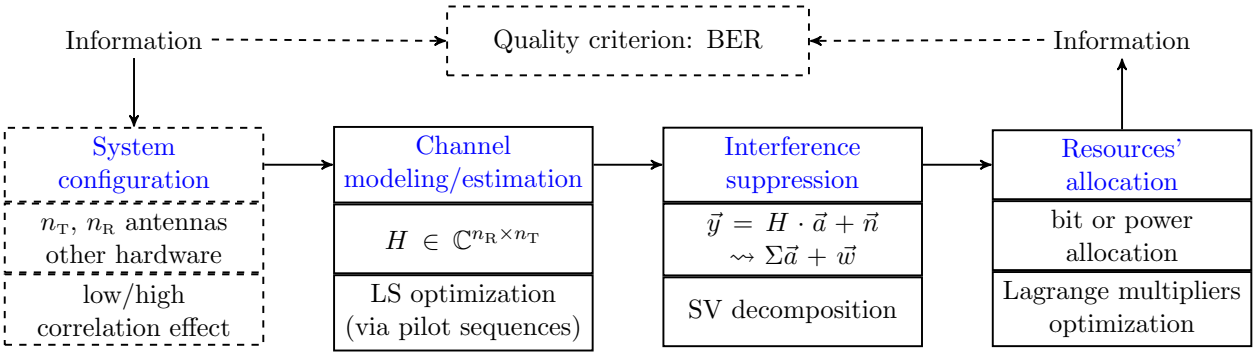

Figure 1. Modeling and simulation of a MIMO digital channel.

An important quality criterion for MIMO links is the bit error ratio (BER), the expectation value of which is characterized by the bit error probability. Among various factors influencing the BER are transmission channel noise (reflected in the linear stochastic model given above) and the interference between the different antenna data streams. Having established the configuration and having estimated the corresponding channel matrix H (cf. Figure 1), we can transform the MIMO link into a number of independent, weighted, frequency flat single-input single-output (SISO) layers using, for instance, singular value decomposition (SVD) to suppress the interference. As a rule, this can be achieved only for an *ideal* H and its SVD (perfect channel state information). The imperfect estimation of the channel coefficients can, in the worst case, lead to a loss of orthogonality in the SVD. It certainly causes a deviation of the ideal weights (or singular values) of the SISO links from the estimated ones and represents a source of uncertainty influencing the BER.

The quality of a MIMO transmission system (with such fixed parameters as the number of transmit and receive antennas, modulation level, and data throughput) can be improved by estimating the channel state more accurately, for example, by using more symbols in training (pilot) sequences (Weikert and Zölzer, 2007). However, the larger the length of such sequences the less data can be put through the channel. For this reason, it is necessary to study the influence of inaccuracy and uncertainty on the achievable transmission quality. To guarantee reliability of a communication with high data rates, the transmission parameters need to be adapted to current channel conditions, for which purpose reliable channel state information is crucial.

The channel matrix and therefore its singular values are influenced by spacial scattering conditions in the MIMO system configuration. The so-called antennas' *correlation effect* appears because of the proximity of the multiple antennas available at the transmitter and receiver sides. In consequence, transmit-to-receive antenna paths become too similar, which decreases the channel capacity and increases the BER. The antennas correlation effect has been extensively studied and analyzed wrt. space diversity possibilities (Lee, 1973; Wang et al., 2009).

For simple MIMO transmission channel and data source models, BER can be computed analytically. It should be as small as possible for the whole link. For quadrature amplitude modulated (QAM) signals, the bit error probability in the general form for a transmission (SISO) layer l is given as

$$P_b^{(l)} = f(M_l) \cdot \operatorname{erfc}\left(g(M_l, \lambda_l, \sigma^2, P_s^{(l)})\right) \quad . \tag{2}$$

Here, f, g are positive-valued functions depending on the constellation size M_l (and the number of bits per symbol $\log_2 M_l$), the noise variance σ^2, the available transmit power per layer $P_s^{(l)}$ and the singular value λ_l corresponding to the considered layer; $\mathrm{erfc}(\cdot)$ is the complementary error function. The weights λ_l are not necessarily equal for each SISO channel, which can be countered by bit and power allocation (BA, PA, resp.). That is, the analytical BER representation can be optimized wrt. the mentioned parameters[1] using, for example, the Lagrange multipliers approach. In poor scattering conditions with high antenna correlation, where the weighting of the SISO channels might turn strongly unequal, such optimization, or the process of bit and power allocation, becomes challenging. A unique indicator of the unequal weighting of the MIMO layers is the ratio ϑ between the smallest and the largest singular value which also characterizes the correlation effect. BER of the correlated system can become significantly higher than that of the uncorrelated one.

After the stage of channel estimation, the process in Figure 1 is influenced by uncertainty in λ_l and σ^2, whereas M_l and $P_s^{(l)}$ can be known exactly or allocated appropriately. For example, (numerical or/and measurement) errors might affect the singular values, which can be assumed to be bounded by the interval $[\ \lambda_l - \varepsilon_l, \lambda_l + \varepsilon_l\ ]$ if the errors are are bounded. From lab simulations, ε_l can be assessed as being up to one order of magnitude smaller than λ_l itself for larger singular values and of the same order of magnitude for small ones. That is, in the linear model in Eq. (1), both stochastic and bounded uncertainty can be present. In (Auer et al., 2018b; Auer and Ahrens, 2020), we employed mixed analytical-numerical strategies relying on methods with automatic result verification to deal with BER minimization under uncertainty in the parameters given above. From the point of view of application, such strategies are of interest, for example, for delay-critical real time interactive voice or video communication systems, where the BER has to be minimized at a fixed data rate under uncertain conditions.

Interval analysis (Moore et al., 2009) and other so-called *methods with result verification* can take into account and propagate bounded uncertainty in parameters directly through an implementation of a mathematical model (provided that the appropriate implementation exists). Moreover, these methods address the question of system reliability by proving formally that the outcome of a simulation implemented on a computer is correct (assuming that the underlying implementation is correct). The results are usually sets of floating point numbers which with certainty contain the exact solution to the model. As a common drawback, the possibility of too wide bounds for the solution sets should be mentioned (e.g., between $-\infty$ and $+\infty$). This drawback is caused by the dependency problem or the wrapping effect (Lohner, 2001). A literature overview and a suggestion for a result verification scheme and dealing with uncertainty using interval analysis in the overall process from Figure 1 are given in (Auer et al., 2018a).

In this paper, we take a closer look at the difference between correlated and uncorrelated systems under uncertainty using the criterion of BER. In general, the performance of MIMO systems is significantly affected by the choice of the number of bits per symbol $\log_2 M_l$ and the appropriate allocation of the transmit power $P_s^{(l)}$ per SISO layer l. A further important factor is the number of activated layers L. To compare the behaviour of correlated and uncorrelated MIMO links, we study the influence of $P_s^{(l)}$, $\log_2 M_l$ and L on them for a fixed throughput. As data, we consider

[1] Note that the noise variance σ^2 is usually considered to be fixed.

two sets for a correlated and an uncorrelated channel with 5000 realizations each (obtained in a lab simulation).

The paper is structured as follows. First, we describe in detail how the data for the comparison we intend to perform are generated, with the focus on channel matrices exhibiting high correlation and on interference suppression, in Section 2. Techniques for channel estimation are to be found, for example, in (Weikert and Zölzer, 2007), and are outside the scope of this paper. In Section 3, we describe approaches to bit and power allocation under bounded uncertainty in parameters, which rely on methods with result verification. A comparison of BA and PA results for the above mentioned channels with low and high correlation is in Section 4. Conclusions and an outlook on future research are in the last section.

2. Correlated Channel Simulation and Interference Suppression

In this section, we describe classical techniques for channel simulation taking into account the correlation effect as well as for interference suppression. They were used to produce the data sets necessary for the comparison in Section 4. Whereas we generated independent and Rayleigh distributed coefficients with equal variance to obtain realizations of the uncorrelated channel matrix, the approach from Section 2.1 was necessary in the case of the correlated MIMO channel. After that, the techniques from Section 2.2 were used for interference suppression. In both cases, MATLAB was employed for implementation.

2.1. MIMO Channel Correlation

While estimating the channel matrix H, it is quite common to assume that its coefficients are independent and Rayleigh distributed with equal variance. However, correlations between the transmit and receive antennas, respectively, cannot be ignored in many cases. The way to include the antenna signal correlation into the MIMO channel model for Rayleigh flat-fading channels is given by (Oestges, 2006) and results in

$$\mathrm{vec}(H) = R_{\mathrm{HH}}^{1/2} \cdot \mathrm{vec}(G) \tag{3}$$

where G is a $(n_{\mathrm{R}} \times n_{\mathrm{T}})$ uncorrelated channel matrix with independent, identically Rayleigh distributed complex elements and $\mathrm{vec}(\cdot)$ being the operator stacking the matrix G into a vector columnwise. The matrix R_{HH} describing the correlation within the channel coefficients $h_{\nu,\mu}$ (with $\nu = 1, \ldots, n_{\mathrm{R}}$ and $\mu = 1, \ldots, n_{\mathrm{T}}$) is defined as

$$R_{\mathrm{HH}} = \mathrm{E}\left\{\mathrm{vec}(H) \cdot \mathrm{vec}(H)^{*\,\mathrm{T}}\right\} \tag{4}$$

with $\mathrm{vec}(H)$ resulting for the example of a system with two transmit and two receive antennas in

$$\mathrm{vec}(H) = \begin{pmatrix} h_{1,1} \\ h_{2,1} \\ h_{1,2} \\ h_{2,2} \end{pmatrix} \quad . \tag{5}$$

Assuming that the correlation introduced by the antenna elements at the transmitter side is independent from the correlation introduced by the antenna elements at the receiver side, the correlation matrix can be defined using the transmitter side correlation matrix R_{TX} and the receiver side correlation matrix R_{RX} as

$$R_{\mathrm{HH}} = R_{\mathrm{TX}} \otimes R_{\mathrm{RX}} \ , \tag{6}$$

where $\otimes$ represents the Kronecker product. For a (2×2) MIMO system, the receiver side correlation matrix R_{RX} is given by

$$R_{\mathrm{RX}}^{(2\times2)} = \begin{pmatrix} \rho_{1,1}^{(\mathrm{RX})} & \rho_{1,2}^{(\mathrm{RX})} \\ \rho_{2,1}^{(\mathrm{RX})} & \rho_{2,2}^{(\mathrm{RX})} \end{pmatrix} = \begin{pmatrix} 1 & \rho^{(\mathrm{RX})} \\ \rho^{*\,(\mathrm{RX})} & 1 \end{pmatrix} \ . \tag{7}$$

The receiver side correlation coefficient can be calculated as

$$\rho_{m,n}^{(\mathrm{RX})} = E\{h_{m,k} \cdot h_{n,k}^{*}\} \ . \tag{8}$$

It describes the correlation between the receive antennas m and n, independent from the transmit antenna k. It should reflect the fact that the value of the correlation coefficient depends on the reference antenna, that is,

$$\rho_{m,n}^{(\mathrm{RX})} = E\{h_{n,k} \cdot h_{m,k}^{*}\} = \rho_{n,m}^{*\,(\mathrm{RX})} \ . \tag{9}$$

Hence, the elements of the correlation matrix symmetric wrt. the main diagonal are complex conjugate. This relationship is due to the sign change in the distance difference between antennas depending on the antenna reference. Similarly, the transmitter-side correlation matrix R_{TX} results in

$$R_{\mathrm{TX}}^{(2\times2)} = \begin{pmatrix} \rho_{1,1}^{(\mathrm{TX})} & \rho_{1,2}^{(\mathrm{TX})} \\ \rho_{2,1}^{(\mathrm{TX})} & \rho_{2,2}^{(\mathrm{TX})} \end{pmatrix} = \begin{pmatrix} 1 & \rho^{(\mathrm{TX})} \\ \rho^{*\,(\mathrm{TX})} & 1 \end{pmatrix} \ . \tag{10}$$

The transmitter side correlation coefficient is obtained as

$$\rho_{k,\ell}^{(\mathrm{TX})} = E\{h_{m,k} \cdot h_{m,\ell}^{*}\} \ . \tag{11}$$

Analogously to the receiver side, it describes the correlation between the transmit antennas k and ℓ, independent from the receive antenna m. Finally, the overall correlation matrix R_{HH} in the example (2×2) system is given by the elements

$$R_{\mathrm{HH}}^{(2\times2)} = \begin{pmatrix} \rho_{1,1,1,1} & \rho_{1,1,1,2} & \rho_{1,2,1,1} & \rho_{1,2,1,2} \\ \rho_{1,1,2,1} & \rho_{1,1,2,2} & \rho_{1,2,2,1} & \rho_{1,2,2,2} \\ \rho_{2,1,1,1} & \rho_{2,1,1,2} & \rho_{2,2,1,1} & \rho_{2,2,1,2} \\ \rho_{2,1,2,1} & \rho_{2,1,2,2} & \rho_{2,2,2,1} & \rho_{2,2,2,2} \end{pmatrix} \tag{12}$$

where $\rho_{k,\ell,m,n}$ are computed as

$$\rho_{k,\ell,m,n} = E\{h_{m,k} \cdot h_{n,\ell}^{*}\} = \rho_{k,\ell}^{(\mathrm{TX})} \cdot \rho_{m,n}^{(\mathrm{RX})} \ . \tag{13}$$

For the model in Equation (3), the square root of the matrix R_{HH} can be computed using Cholesky decomposition as $R_{\mathrm{HH}}^{1/2} = \left(R_{\mathrm{TX}}^{1/2} \otimes R_{\mathrm{RX}}^{1/2}\right)$.

2.2. Interference Suppression

Having generated the channel matrix H, we decompose it as $H = U \cdot \Sigma \cdot V^\dagger$, where U and V are unitary matrices, Σ is the diagonal matrix with real elements and $V^\dagger$ denotes the Hermitian adjoint of V. The matrix Σ contains the positive square roots of the eigenvalues ξ_l of $H^\dagger H$ in descending order on the main diagonal (singular values denoted by $\lambda_l = \sqrt{\xi_l}$ throughout the paper). If a pre-processed data vector $\vec{x} := V \cdot \vec{a}$ is considered and the corresponding receive signal $\vec{z} := H\vec{x} + \vec{n}$ is post-processed by $U^\dagger$, then the new receive signal is

$$\vec{u} := U^\dagger \vec{z} = U^\dagger \left(U \Sigma V^\dagger \right) V\vec{a} + U^\dagger \vec{n} = \Sigma \vec{a} + \vec{w} \ , \tag{14}$$

where the vector $\vec{a}$ is the transmitted signal vector and $\vec{n}$ is the Gaussian noise vector as explained in the Introduction. In this way, the MIMO link is transformed (ideally) into $L = \min\{n_\mathrm{T}, n_\mathrm{R}\}$ independent, non-interfering SISO layers u_l having (unequal) weights λ_l:

$$u_l = \lambda_l a_l + w_l \quad \text{for} \quad l = 1 \ldots L \ . \tag{15}$$

There are a number of difficulties during this stage due to numerics or uncertainty. For example, $U^\dagger \cdot U$ or $V^\dagger \cdot V$ are not exactly identity matrices because of numerical errors, which might create interference between the SISO links. Moreover, the elements of the matrix H can never be obtained perfectly in a real life situation. That is, H includes bounded uncertainty in its elements in addition to the stochastic one modeled by the Rayleigh distribution, making the weights λ_l also uncertain.

The possibilities to apply methods with result verification (or other set-based techniques) to SVD under the assumption of bounded uncertainty in H are limited. It is possible to obtain (verified) bounds on (real) singular values of H (Deif, 1991; Li and Chang, 2003; Su et al., 2011; Hladík et al., 2010; Rump, 2011). However, the interval equivalents of matrices U and V do not convey the same meaning as their floating-point counterparts as explained in (Kearfott, 1996). This prohibits any kind of set-based decomposition in the manner given by Eq. (14) and (15). (Note that as long as the matrices themselves are not needed, the bounds for λ_l can be used in the same way as in Eq. (15).) However, a MIMO link can be also decomposed into several SISO links based on the geometric mean decomposition (Ahrens et al., 2016), the study of which from the point of view of verified techniques is a subject of our future work. In this paper, we take lowest and highest values for each λ_l from the lab simulation data. Note that the proposed approach would work according to the same principles with the analytical bounds. Additionally, since the number of simulations is moderately large (5000) and the model in Eq. (1) takes into account the Gaussian noise, bounds for λ_l based on these data should not be too far from the analytical or real life values.

2.3. Comparison of Correlated and Uncorrelated Channel Realizations

Due to the proximity of the antennas at the transmitter and the receiver side, the unequal weighting of the MIMO layers can become stronger (antennas correlation effect as described in the Introduction). The ratio ϑ between the smallest and the largest singular values can be considered as the unique indicator of the unequal weighting of the MIMO layers. In Figure 2, the frequencies of occurrence for the values of the weighting factor ϑ are shown for the example of an uncorrelated

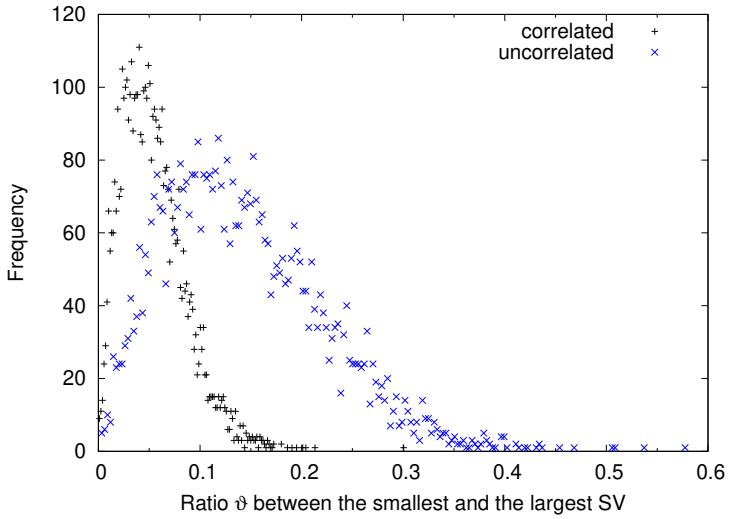

Figure 2. Frequencies of values for the ratio ϑ for uncorrelated ($\times$) and correlated ($+$) frequency flat (4×4) MIMO channel.

and a correlated frequency flat (4×4) MIMO system. (The corresponding frequencies for the amplitudes of the values are shown in Figure 3.) Figure 3 demonstrates how the difference between the largest and the smallest singular values (i. e., the unequal weighting) increases for the correlated system. This means that the ratio between the smallest and the largest singular value decreases as the correlation increases, which can be observed from Figure 2. That is, the probability of having predominant layers also increases. As a result, the use of resource allocation techniques seems an appropriate solution to optimize the layer behavior. It seems that no power should be allocated to the MIMO layer having the smallest singular value because the overall performance would be deteriorated. This claim is substantiated and extended in Section 4.

3. Guaranteed BER Minimization Through Power and Bit Allocation

After the SISO weights λ_l are computed for a given MIMO link, it is necessary to think about how to minimize its overall BER. In this Section, we describe possibilities for power and bit allocation under uncertainty in in the weights. In (Auer and Ahrens, 2020), more information is given on this overall subject and, in particular, on possibilities to minimize wrt. other parameters. Additionally, the number of activated layers $L \leq \min\{n_\mathrm{T}, n_\mathrm{R}\}$ might play an important role. Not every layer $l \in \{1, \ldots, L\}$ of the MIMO link should necessarily be active to achieve the best performance. In Section 4, we consider possible choices for active layers in detail. Here, we assume that L is fixed within a certain suitable range.

3.1. Enclosing the BER for Uncertain Parameters

We work with the following formula to compute the the overall BER (for derivation, see, for example, (Auer et al., 2018b)):

$$P_b = \frac{2}{\sum_{l=1}^{L} \log_2 M_l} \sum_{l=1}^{L} \left(1 - \frac{1}{\sqrt{M_l}}\right) \cdot \operatorname{erfc}\left(\frac{\lambda_l}{2\sigma}\sqrt{\frac{3 \cdot P_s}{L(M_l - 1)}}\right) \quad , \tag{16}$$

with P_s being the overall available transmit power. The coefficient $\dfrac{2}{\sum_{l=1}^{L} \log_2 M_l}$ is constant for a fixed throughput and is independent of the number of effectively activated layers.

From Eq. (16), it is evident that the major charasteristics influencing the BER are the singular values (layer weights), the noise variance and the number of bits per symbol. Initially, the transmit power per layer $P_s^{(l)} = P_s/L$ is supposed to be equal for each layer. As shown in (Auer and Ahrens, 2020), if $\lambda_l \in [\ \underline{\lambda}_l, \overline{\lambda}_l\ ]$, where $\underline{\lambda}_l$, $\overline{\lambda}_l$ are known lower and upper bounds, respectively, and the standard deviation $\sigma \in [\ \underline{\sigma}, \overline{\sigma}\ ]$, then a conservative upper bound on the BER can be obtained as

$$P_b(\sigma, \lambda_1 \dots \lambda_L) \leq \frac{2}{\sum_{l=1}^{L} \log_2 M_l} \sum_{l=1}^{L} \left(1 - \frac{1}{\sqrt{M_l}}\right) \cdot \operatorname{erfc}\left(\frac{\underline{\lambda}_l}{2\overline{\sigma}}\sqrt{\frac{3P_s}{L(M_l - 1)}}\right) \quad . \tag{17}$$

That means that, due to monotonicity of the involved functions, it is not necessary to work with actual ranges but with their bounds only, which makes verified optimization easier.

3.2. Power Allocation

If the number of transmitted bits per layer is fixed, a possible approach to BER minimization is the power allocation technique assigning more power to the layers with small weights. This becomes necessary because small λ_l lead to large values of bit error probability $P_b^{(l)}$ per MIMO layer l since $\operatorname{erfc}(\cdot)$ is monotonically decreasing with λ_l. If the Lagrange multipliers method is used, then the following cost function needs to be minimized:

$$\begin{aligned} J(\pi_1 \dots \pi_L, \mu) \ = \ & \frac{2}{\sum_{l=1}^{L} \log_2 M_l} \sum_{l=1}^{L} \left(1 - \frac{1}{\sqrt{M_l}}\right) \\ & \cdot \ \operatorname{erfc}\left(\frac{\pi_l \lambda_l}{2\sigma}\sqrt{\frac{3 \cdot P_s}{L(M_l - 1)}}\right) + \mu \left(\sum_{l=1}^{L} \pi_l^2 - L\right) \longrightarrow \min, \end{aligned} \tag{18}$$

where $\pi_1 > 0, \dots, \pi_L > 0$ are the power allocation parameters with which we modify the weights λ_l from Eq. (15) in order to improve P_b from Eq. (16) and μ is the Lagrange multiplier assigned to

the constraint $\sum_{l=1}^{L} \pi_l^2 = L$. With the notations

$$k_l = k_l(M_1 \dots M_L) \;:=\; \frac{2}{\sum_{l=1}^{L} \log_2 M_l} \cdot \left(1 - \frac{1}{\sqrt{M_l}}\right), \tag{19}$$

$$c_l = c_l(M_l, \sigma, P_s, L) \;:=\; \frac{1}{2\sigma}\sqrt{\frac{3 \cdot P_s}{L(M_l - 1)}},\; l = 1...L\;, \tag{20}$$

the Lagrange multipliers approach produces the nonlinear system of equations (21) for stationary points of the cost function (18) :

$$\frac{\partial J(\pi_1 \dots \pi_L, \mu)}{\partial \pi_l} = -\frac{2k_l}{\sqrt{\pi_l}}\left(c_l \lambda_l e^{-c_l^2 \lambda_l^2 \pi_l^2}\right) + 2\mu\pi_l = 0, \quad \sum_{l=1}^{L} \pi_l^2 - L = 0\;, \tag{21}$$

where $\pi_l > 0, l \in \{1, \dots, L\}$. Moreover, it is clear from the first L equations that μ must be positive.

The second derivative $\dfrac{\partial^2 J}{\partial \pi_l \partial \pi_m} = 0$ for $l \neq m$ and is positive for $l = m$. The bordered Hessian is symmetric and has the form

$$\begin{pmatrix} 0 & 2\pi_1 & \cdots & 2\pi_L \\ 2\pi_1 & 2\mu + \dfrac{4k_1 c_1^2 \lambda_1^2}{\sqrt{\pi_1}} \pi_1 e^{-c_1^2 \lambda_1^2 \pi_1^2} & \cdots & 0 \\ 2\pi_2 & 0 & \cdots & 0 \\ \vdots & \vdots & \ddots & \vdots \\ 2\pi_L & 0 & \cdots & 2\mu + \dfrac{4k_L c_L^2 \lambda_L^2}{\sqrt{\pi_L}} \pi_L e^{-c_L^2 \lambda_L^2 \pi_L^2} \end{pmatrix}$$

The determinants of all relevant $L - 1$ leading principal minors have the structure

$$(l+1) \times (l+1): \qquad \begin{vmatrix} 0 & a_1 & \cdots & a_l \\ a_1 & d_1 & \cdots & 0 \\ \vdots & & \ddots & \\ a_l & 0 & \cdots & d_l \end{vmatrix} = -\sum_{i=1}^{l} \left(a_i^2 \prod_{k=1, k\neq i}^{l} d_k \right)$$

for $l = 2 \dots L$. The elements d_k are positive for $\pi_k > 0$ $(k = 1 \dots l)$, $\mu > 0$, that is, the determinants are always negative. For one constraint, this means that a stationary point is a local minimum. Using a solver for systems of non-linear equations based on methods with result verificaiton (e.g., C-XSC Toolbox (Hofschuster et al., 2008)), we can compute a guaranteed enclosure for it from the system in Eq. (21). Working in a verified way has the advantages of taking care of numerical errors and of the possibility to prove the uniqueness of the solution (leading to the proof that the minimum is global) on a computer.

3.3. Influence of Bits per Symbol

The number of bits per transmitted symbol and layer influences the overall BER. For example, we studied the case of $M_1 = M_2 = 16$ and $M_1 = 64$, $M_2 = 4$ for the (4×4) MIMO system with a fixed throughput of 8 bit/s/Hz and two active layers in (Auer et al., 2018b). The latter case had a better BER for the same signal-to-noise ratio (SNR) and MIMO links with both high and low correlation coefficients. Therefore, it is necessary to determine optimal constellations (possibly, under additional consideration of power allocation).

The optimization with respect to bits per symbol is complicated by the fact that M_l should be positive integer powers of 2 fitting the desired throughput, which leads to a non-linear mixed-integer programming problem (Lee and Leyffer, 2011). The BER to minimize is

$$P_b(M_1 \dots M_L) = \frac{2}{T} \sum_{l=1}^{L} \left(1 - \frac{1}{\sqrt{M_l}}\right) \cdot \operatorname{erfc}\left(\frac{\hat{c}_l}{\sqrt{M_l - 1}}\right) \longrightarrow \min \quad \text{s.t.} \quad \sum_{l=1}^{L} \log_2 M_l = T, \tag{22}$$

where $\hat{c}_l = \hat{c}_l(\lambda_l, \pi_l, \sigma, P_s, L) := \dfrac{\lambda_l \pi_l}{2\sigma} \sqrt{\dfrac{3P_s}{L}}$ and T the desired throughput. The problem can be solved for small T by a brute force (trial and error) approach using every admissible positive integer solution to the problem in Eq. (22). This is the case for a fixed throughput of 8 bit/s/Hz we consider in the next section. In general, it is necessary to augment the approach by a branch and bound algorithm.

4. Numerical Results: BER Optimization for a Correlated and Uncorrelated Wireless MIMO Link with Four Antennas

In this section, we illustrate the ideas using a practical problem. We consider a correlated and uncorrelated wireless frequency flat MIMO link with $n_{\mathrm{T}} = n_{\mathrm{R}} = 4$ antennas. The desired throughput is 8 bit/s/Hz and the available transmit power $P_s = 1\mathrm{W}$ throughout the simulations.

4.1. Simulation Settings

Two data sets with 5000 elements (channel realizations) each were obtained for both variants of the wireless channel in a non-verified simulation with $\delta^2 = \frac{1}{2}$ as described in Sections 2.1, 2.2 (data available on demand via email). The correlation coefficients at the transmitter and receiver sides were chosen as $\rho^{(\mathrm{RX})} = \rho^{(\mathrm{TX})} = 0.2375$. From Figure 2, it can be seen that the ratio ϑ for the correlated channel is significantly lower in the produced data sets. The frequencies of occurrence for the amplitudes of all four singular values are shown in Figure 3.

We provide numerical results for the SNR of $\left(\frac{E_s}{N_0}\right)_{\mathrm{dB}} = 10$ dB, where E_s denotes the symbol energy and N_0 the noise power spectral density with the corresponding value for σ computed as $\sigma = \sqrt{\dfrac{P_s}{2 \cdot \exp\left(\frac{\ln 10}{10} \cdot \left(\frac{E_s}{N_0}\right)_{\mathrm{dB}}\right)}} = \sqrt{\frac{1}{20}} \approx 0.2236$. All the following simulations are performed with result verification using C-XSC Toolbox (Hofschuster et al., 2008). The shown bounds are rounded

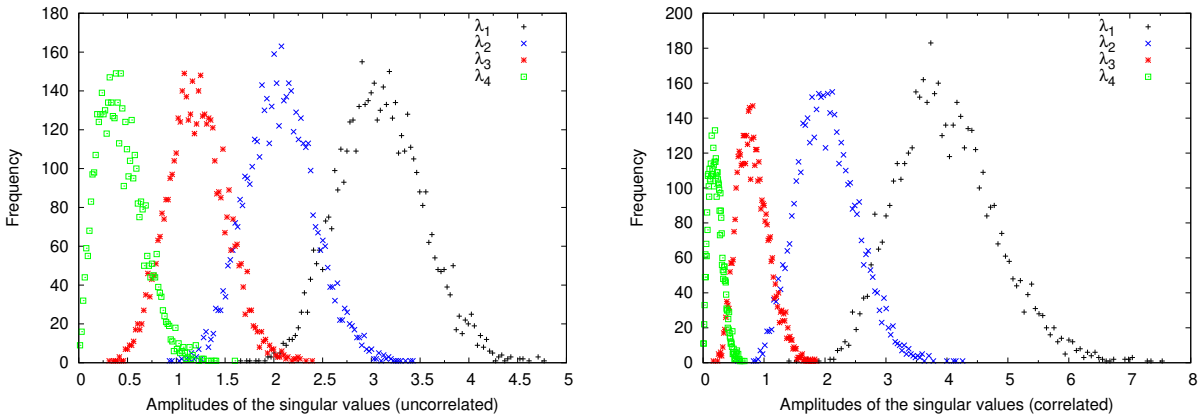

Figure 3. Amplitudes of the singular values in the considered data sets for the uncorrelated (left) and the correlated (right) channels.

outwards to the fourth digit after the decimal point; the actual interval widths are somewhat smaller. In practice, it is accurate enough to store the data up to the fourth digit after the decimal point since the changes in digits in places after that do not have much influence on the overall system. If the widths of enclosures are small, we reproduce only one (rounded) value.

4.2. Power and Bit Allocation

The lower bounds for λ_i for the data set in the uncorrelated case are $\underline{\lambda}_1 = 2.4208$, $\underline{\lambda}_2 = 0.9180$, $\underline{\lambda}_3 = 0.3022$, $\underline{\lambda}_4 = 0.0049$. The correlation coefficient for these bounds is $\vartheta \approx 20 \times 10^{-4}$, with the worst possible one from the data set equal to approx. 18×10^{-4}. That is, the upper bound for the BER at 10 dB for this system with all four layers active and $M_1 = 4$, $M_2 = 4$, $M_3 = 4$ and $M_4 = 4$ is 0.2217 (the outer bound). The power allocation reduces it to the value of 0.1974. The lower singular value bounds in the correlated case are $\underline{\lambda}_1 = 1.3791$, $\underline{\lambda}_2 = 0.5526$, $\underline{\lambda}_3 = 0.1609$, $\underline{\lambda}_4 = 0.0013$ ($\vartheta \approx 9.4 \times 10^{-4}$, the worst from the data set 2.5×10^{-4}). Here, the upper bound on the BER under the same conditions is 0.2761, reduced to 0.2553 by PA, that is, significantly higher than in the uncorrelated case. Note that the actual worst case BER for the simulated data are 0.1909 and 0.2180, respectively. That is, the bounds obtained with interval arithmetic are conservative. In Figure 4, the BER with and without power allocation is shown for each crisp set of 5000 λ_l values in both the uncorrelated (left) and correlated (right) case for $L = 4$. For better presentation, only every 100th data point is plotted. It can be seen that the BER is worse for the correlated case.

In general, the BER is the worst in both the correlated and uncorrelated case if all four MIMO layers are active as can be seen from Table I. Especially, the choice of $M_1 = 4$, $M_2 = 4$, $M_3 = 4$ and $M_4 = 4$ (number 14 in the Table) is unfavorable for both systems' BER. In the Table, the results of optimization wrt. the transmission power, the number of bits per symbol and the number of active layers at 10 dB are shown for the uncorrelated and correlated case as intervals with the best and worst possible bound from the respective data sets. The best constellations are highlighted in bold face, with the second-best shown in italics. Since the $\lambda_1 \geq \lambda_2 \geq \lambda_3 \geq \lambda_4$, putting more

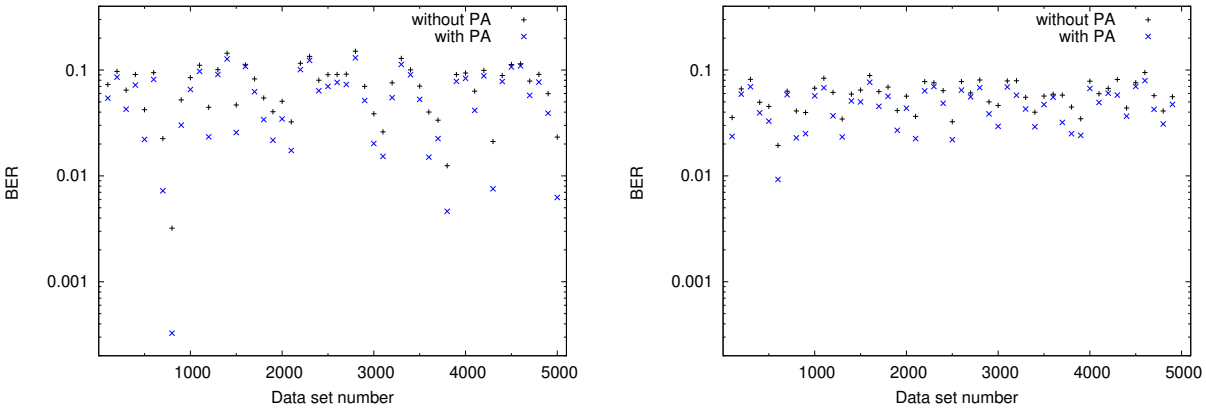

Figure 4. BER with and without power allocation for 5000 possibilities for λ_l (at 10 dB) in the uncorrelated (left) and correlated (right) case with active four layers and $M_1 = 4$, $M_2 = 4$, $M_3 = 4$, $M_4 = 4$.

symbols through the weaker layers does not improve the BER so that only the situations where $M_1 \geq M_2 \geq M_3 \geq M_4$ need to be considered.

The Table is consistent with the knowledge that correlated MIMO systems have a higher BER. Moreover, we can notice that the power allocation technique does not reduce the BER as much in the correlated case as in the uncorrelated one. Additionally, we can conclude that the number of active layers for these (4×4) MIMO systems needs to be either two or three, since they result in the best BER in both cases. Almost every choice of symbols per layer with $L = 2$ and $L = 3$ results in a good BER in the uncorrelated case aside from the marginal cases $M_1 = 128$, $M_2 = 2$ and $M_1 = 64$, $M_2 = 2$, $M_3 = 2$ (with $M_1 = 32$, $M_2 = 8$; $M_1 = 16$, $M_2 = 8$, $M_3 = 2$ or $M_1 = 32$, $M_2 = 4$, $M_3 = 2$ being the best constellations). In the correlated case, the resource allocation plays a more important role since only two constellations lead to a good BER, namely, $M_1 = 32$, $M_2 = 8$ and $M_1 = 32$, $M_2 = 4$, $M_3 = 2$.

5. Conclusions

In this paper, we presented a comparison of correlated and uncorrelated MIMO systems from the point of view of resource allocation. For this purpose, we relied on examples of corresponding (4×4) links with 5000 channel realisations each obtained from MATLAB simulations. Note that the resource allocation was performed with result verification, that is, the achieved minima are proved to be unique. We studied both MIMO systems wrt. power and bit allocation as well as wrt. the number of active layers. The important conclusions are:

— All four layers should never be activated at the same time, that is, the weakest layer should be switched off;

— For correlated systems, the resource allocation plays an especially important role; as a rule, working with two active layers results in the best performance for the BER.

Table I. Analysis of BER for 5000 channel realizations at 10 dB with throughput of 8 bit/s/Hz (high and low correlation, with and without power allocation).

	Layer M_1,M_2,M_3,M_4	BER (correlated)	BER-PA (correlated)	BER (uncorrelated)	BER-PA (uncorrelated)
			One active layer		
1	256, 0, 0, 0	[0.0023,0.1492]	the same	[0.0240, 0.13423]	the same
			Two active layers		
2	128, 2, 0, 0	[0.0022,0.1449]	[0.0001,0.1220]	[0.0232, 0.1304]	[0.0059, 0.1036]
3	64, 4, 0, 0	[$55{\cdot}10^{-6}$,0.1103]	[$4{\cdot}10^{-6}$,0.0959]	[0.0044, 0.0928]	[0.0007, 0.0749]
4	32, 8, 0, 0	**[$10{\cdot}10^{-7}$,0.0808]**	**[$2{\cdot}10^{-7}$,0.0773]**	**[0.0002, 0.0599]**	*[0.0001, 0.0556]*
5	16, 16, 0, 0	[$40{\cdot}10^{-7}$,0.1092]	[$3{\cdot}10^{-7}$,0.0981]	[$1.4{\cdot}10^{-4}$, 0.06710]	[$1.1{\cdot}10^{-4}$, 0.0589]
			Three active layers		
6	64, 2, 2, 0	[$8{\cdot}10^{-4}$,0.1279]	[$8{\cdot}10^{-6}$,0.1002]	[0.0127, 0.1121]	[0.0009, 0.0771]
7	32, 4, 2, 0	*[$12{\cdot}10^{-6}$,0.0926]*	*[$2{\cdot}10^{-6}$,0.0775]*	[0.0015, 0.0739]	**[$6{\cdot}10^{-5}$, 0.0533]**
8	16, 8, 2, 0	[$11{\cdot}10^{-6}$,0.1006]	[$5{\cdot}10^{-6}$,0.0936]	*[0.0001, 0.06417]*	[$2{\cdot}10^{-5}$, 0.0584]
9	16, 4, 4, 0	[$11{\cdot}10^{-5}$,0.1015]	[$1{\cdot}10^{-5}$,0.0972]	[$9{\cdot}10^{-5}$, 0.0850]	[$1{\cdot}10^{-5}$, 0.0785]
10	8, 8, 4, 0	[0.0001,0.1429]	[$7{\cdot}10^{-5}$,0.1282]	[$2{\cdot}10^{-5}$, 0.1048]	[$1{\cdot}10^{-5}$, 0.0916]
			Four active layers		
11	32, 2, 2, 2	[0.0106,0.1532]	[0.0032,0.1255]	[0.0073, 0.1426]	[0.0005, 0.1129]
12	16, 4, 2, 2	[0.0071,0.1252]	[0.0023,0.1181]	[0.0006, 0.1099]	[$7{\cdot}10^{-5}$, 0.1010]
13	8, 4, 4, 2	[0.0109,0.1665]	[0.0038,0.1529]	[$7{\cdot}10^{-5}$, 0.1419]	[$4{\cdot}10^{-5}$, 0.1344]
14	4, 4, 4, 4	[0.0414,0.2180]	[0.0228,0.2028]	[0.0014, 0.1909]	[0.0002, 0.1785]

However, we did not consider explicitly the influence of the noise variance σ^2 on the results. All simulations were performed for the SNR of 10 dB. To study this influence is a subject of our future work.

References

Ahrens, A., Benavente-Peces, C., and Cano-Broncano, F. (2016). Power Allocation in SVD- and GMD-assisted MIMO Systems. *Optimization and Engineering*.

Auer, E. and Ahrens, A. (2020). Guaranteed Minimization of the Bit Error Ratio for MIMO Systems: A Mathematical Viewpoint. *ASCE-ASME Journal of Risk and Uncertainty in Engineering Systems Part B: Mechanical Engineering*. accepted.

Auer, E., Ahrens, A., Sandman, A., and Benavente-Peces, C. (2018a). Influence of uncertainty and numerical errors in the context of MIMO systems. In *8th International Workshop on Reliable Engineering Computing*, pages 21–30.

Auer, E., Benavente-Peces, C., and Ahrens, A. (2018b). Solving the Power Allocation Problem Using Methods with Result Verification. *Int. J. Reliability and Safety*, 12(1/2):86–102.

Deif, A. (1991). Singular values of an interval matrix. *Linear Algebra and its Applications*, 151:125 – 133.

Foschini, G. (1996). Layered space-time architecture for wireless communication in a fading environment when using multi-element antennas. *Bell Labs Technical Journal*, 1(2):41 – 59.

Hladík, M., Daney, D., and Tsigaridas, E. P. (2010). Bounds on real eigenvalues and singular values of interval matrices. *SIAM Journal of Matrix Analysis and Applications*, 31(4):2116–2129.

Hofschuster, W., Krämer, W., and Neher, M. (2008). C-XSC and Closely Related Software Packages. In Cuyt, A. M., Krämer, W., Luther, W., and Markstein, P. W., editors, *Numerical Validation in Current Hardware Architectures LNCS 5492*, pages 68–102.

Kearfott, R. B. (1996). *Rigorous Global Search: Continuous Problems*. Kluwer.

Lee, J. and Leyffer, S. (2011). *Mixed Integer Nonlinear Programming*. Springer Publishing Company, Incorporated.

Lee, W.-Y. (1973). Effects on Correlation between two Mobile Radio Base-Station Antennas. *IEEE Transactions on Vehicular Technology*, 22(4):130–140.

Li, W. and Chang, Q. (2003). Inclusion intervals of singular values and applications. *Computers & Mathematics with Applications*, 45(10):1637–1646.

Lohner, R. (2001). On the Ubiquity of the Wrapping Effect in the Computation of Error Bounds. In Kulisch, U., Lohner, R., and Facius, A., editors, *Perspectives on Enclosure Methods*, pages 201–218. Springer-Verlag.

Moore, R. E., Kearfott, R. B., and Cloud, M. J. (2009). *Introduction to Interval Analysis*. Society for Industrial and Applied Mathematics, Philadelphia.

Oestges, C. (2006). Validity of the Kronocker Model for MIMO Correlated Channels. In *Vehicular Technology Conference*, volume 6, pages 2818–2822, Melbourne.

Raleigh, G. G. and Cioffi, J. M. (1998). Spatio-Temporal Coding for Wireless Communication. *IEEE Transactions on Communications*, 46(3):357–366.

Rump, S. M. (2011). Verified bounds for singular values, in particular for the spectral norm of a matrix and its inverse. *BIT Numerical Mathematics*, 51(2):367–384.

Sklar, B. (1997). Rayleigh fading channels in mobile digital communication systems. I. Characterization. *IEEE Communications Magazine*, 35(7):90–100.

Su, F., Xu, Z., Dong, Q., and Li, H. (2011). Bounds analysis of singular values for real symmetric interval matrices. *International Journal of Research and Reviews in Applied Sciences*, 6(4):391 – 391.

Telatar, I. E. (1999). Capacity of multi-antenna Gaussian channels. *EUROPEAN TRANSACTIONS ON TELECOMMUNICATIONS*, 10:585–595.

Wang, H., Wang, P., Ping, L., and Lin, X. (2009). How Does Correlation Affect the Capacity of MIMO Systems with Rate Constraints? In *IEEE Global Telecommunications Conference (GLOBECOM)*, pages 1–5.

Weikert, O. and Zölzer, U. (2007). Efficient MIMO Channel Estimation With Optimal Training Sequences. In *Proceedings of 1st Workshop on Commercial MIMO Components and Systems*, Duisburg, Germany.